FEBS Letters 585 (2011) 307–312

journal homepage: www.FEBSLetters.org

Crystal structures of LacD from *Staphylococcus aureus* and LacD.1 from *Streptococcus pyogenes*: Insights into substrate specificity and virulence gene regulation

Sang Jae Lee [a], Hyoun Sook Kim [a], Do Jin Kim [a], Hye-Jin Yoon [a], Kyoung Hoon Kim [a], Ji Young Yoon [a], Se Won Suh [a,b,*]

[a] Department of Chemistry, College of Natural Sciences, Seoul National University, Seoul 151-742, Republic of Korea
[b] Department of Biophysics and Chemical Biology, College of Natural Sciences, Seoul National University, Seoul 151-742, Republic of Korea

ARTICLE INFO

Article history:
Received 3 July 2010
Revised 29 November 2010
Accepted 22 December 2010
Available online 28 December 2010

Edited by Christian Griesinger

Keywords:
Tagatose-1,6-bisphosphate aldolase
LacD
LacD.1
Crystal structure
Staphylococcus aureus
Streptococcus pyogenes

ABSTRACT

***Staphylococcus aureus* LacD, a Class I tagatose-1,6-bisphosphate (TBP) aldolase, shows broadened substrate specificity by catalyzing the cleavage of 1,6-bisphosphate derivatives of D-tagatose, D-fructose, D-sorbose, and D-psicose. LacD.1 and LacD.2 are two closely-related Class I TBP aldolases in *Streptococcus pyogenes*. Here we have determined the crystal structures of *S. aureus* LacD and *S. pyogenes* LacD.1. Monomers of both enzymes are folded into a $(\beta/\alpha)_8$ barrel and two monomers associate tightly to form a dimer in the crystals. The structures suggest that the residues E189 and S300 of rabbit muscle Class I fructose-1,6-bisphosphate (FBP) aldolase are important for substrate specificity. When we mutated the corresponding residues of *S. aureus* LacD, the mutants (L165E, L275S, and L165E/L275S) showed enhanced substrate specificity toward FBP.**

Structured summary:
lacD binds to **lacD** by X-ray crystallography (View interaction)
lacD1 binds to **lacD1** by X-ray crystallography (View interaction)

1. Introduction

Two mechanistically distinct aldolases (Class 1 and Class II) have been found in both prokaryotic and eukaryotic organisms [1]. Catalysis by Class I aldolases occurs via a covalent Schiff-base intermediate, whereas Class II aldolases utilize a divalent metal ion (Zn^{2+} or Fe^{2+}) for catalysis [1,2]. Class I fructose-1,6-bisphosphate (FBP) aldolases from vertebrate animals have been well-characterized. They are tetrameric and a conserved carboxy-terminal tyrosine residue is required for their catalytic activity [1]. Class II aldolases are found in bacteria and yeast [1,2]. Archaea have been shown to use both Class I and Class II aldolases [1,3]. No obvious sequence similarity exists between the two classes of aldolases [1].

Compared to Class I FBP aldolases that catalyze a highly stereospecific reaction toward FBP, *Staphylococcus aureus* LacD was shown to have broadened substrate specificity by catalyzing the cleavage of 1,6-bisphosphate derivatives of D-tagatose, D-fructose, D-sorbose, and D-psicose [4]. These four D-2-ketohexose-1,6-bisphosphates differ in stereochemistry with respect to their hydroxyl groups at carbon atoms 3 and 4 of the hexose (Supplementary Fig. S1). The substrate specificity of tagatose-1,6-bisphosphate (TBP) aldolases was therefore expected to be directed at hexose carbon atoms 1, 2, 5, and 6 only [5].

Streptococcus pyogenes (group A streptococcus; GAS), a Gram-positive bacterial pathogen, causes an exceptionally broad range of infections from pharyngitis and impetigo, to necrotizing fasciitis, streptococcal toxic shock syndrome, and post-infection immune sequelae [6,7]. GAS must adapt to various niches which they encounter in the human host. Compared to human blood, glucose levels at other common sites of streptococcal infection are generally quite low, meaning that alternative energy sources need to be pursued [8]. Therefore, regulatory elements must respond to environmental signals and control the expression of virulence genes [6]. There are multiple levels of regulatory links between virulence factor production and complex carbohydrate catabolism in GAS, demonstrating the close relationship between carbohydrate utilization and streptococcal pathogenesis [8]. This makes understanding of the regulation of carbohydrate utilization and its relation to virulence gene expression in *S. pyogenes* an important step toward the discovery of antibacterial therapeutics against *S. pyogenes*.

Abbreviations: GAS, group A streptococcus; TBP, tagatose-1,6-bisphosphate; FBP, fructose-1,6-bisphosphate; R.M.S.D., root mean square deviation; DHAP, dihydroxyacetone phosphate

* Corresponding author at: Department of Chemistry, College of Natural Sciences, Seoul National University, Seoul 151-742, Republic of Korea. Fax: +82 2 8891568.
E-mail address: sewonsuh@snu.ac.kr (S.W. Suh).

0014-5793/$36.00 © 2010 Federation of European Biochemical Societies. Published by Elsevier B.V. All rights reserved.
doi:10.1016/j.febslet.2010.12.038

In *S. pyogenes*, two closely-related Class I TBP aldolases, i.e., LacD.1 and LacD.2, exist. These two enzymes are highly homologous to each other, with a sequence identity of 72%. Both are catalytically active [9]. Interestingly, however, only one of them (LacD.1) has an additional regulatory function on the transcription of virulence genes, linking nutritional status to transcription of virulence genes [9–11]. *S. pyogenes* RopB, an Rgg family transcription regulator, influences the production of proteins during transition to the stationary phase [10]. RopB was shown to associate with its negative regulator LacD.1, which may be a mechanism for maintaining temporally controlled gene expression programs [10,11].

To provide structural basis for understanding the substrate specificity of *S. aureus* LacD and the regulatory role of *S. pyogenes* LacD.1, we have determined their crystal structures. These structures suggest that the residues E189 and S300 of rabbit muscle FBP aldolase are important for substrate specificity. When we mutated the corresponding residues of *S. aureus* LacD, the mutants (L165E, L275S, and L165E/L275S) showed enhanced substrate specificity toward FBP. Thus, our work provides structural insights into the broadened substrate specificity of Class I TBP aldolases. The dimeric structure of *S. pyogenes* LacD.1 has some implications for its specific association with the Rgg family transcription regulator RopB.

2. Materials and methods

2.1. Cloning, protein expression, and purification

Details of cloning, expression, and purification of LacD from *S. aureus* and LacD.1 from *S. pyogenes* are described in the Supplementary data. Briefly, they were expressed from a pET-21a(+) expression plasmid (Novagen) in *Escherichia coli* Rosetta2(DE3) cells. C-terminal His-tagged polypeptides were purified by nickel-affinity chromatography, anion exchange chromatography on a HiTrap-Q column, and size exclusion chromatography on a Superdex 200 column.

2.2. Crystallization, structure determination, and refinement

The crystallization conditions and structure determination using the single wavelength anomalous dispersion method as well as refinement are described in the Supplementary data. The selenomethionine-substituted crystals of *S. aureus* LacD and native crystals of *S. pyogenes* LacD.1 were grown using the sitting-drop vapor diffusion method at 14 °C. The coordinates and structure factors have been deposited in the Protein Data Bank under accession codes 3MYP for *S. aureus* LacD and 3MYO for *S. pyogenes* LacD.1, respectively.

2.3. TBP/FBP cleavage assays

Details of the TBP/FBP cleavage assays are described in the Supplementary data. Briefly, coupled enzyme assays using glycerol-3-phosphate dehydrogenase and triose-phosphate isomerase were used to determine the TBP/FBP cleavage activity. The assays were performed at 30 °C and the decrease in absorbance at 340 nm was measured.

3. Results and discussion

3.1. Overall monomer structures and comparison of monomer structures

The refined model of *S. aureus* LacD accounts for 1284 amino acid residues in four monomers in the asymmetric unit. Six residues (M1–S3 and R325–K326) and the C-terminal fusion tag are disordered in all four chains. The model of *S. pyogenes* LacD.1 accounts for 656 amino acid residues in two monomers. In this model, Met1 and four histidines of the C-terminal fusion tag are disordered in both polypeptide chains. Refinement statistics are given in Supplementary Table 1. *S. aureus* LacD and *S. pyogenes* LacD.1 monomers have identical overall folding, which comprises a $(\beta/\alpha)_8$ barrel in the order β1–α3–β2–α4–β3–α5–β4–α6–β5–α7–β6–α8–β7–α9–β8–α11 (Fig. 1A). The helix α1 covers one face of the $(\beta/\alpha)_8$ barrel; α2 and α10 are positioned next to α11, stretching away from the $(\beta/\alpha)_8$ barrel.

Four *S. aureus* LacD monomers in the asymmetric unit are highly similar to each other, with a root mean square deviation (R.M.S.D.) of 0.42–0.76 Å for 285–304 Cα atom pairs. Two monomers of *S. pyogenes* LacD.1 in the asymmetric unit are also highly similar to each other, with a R.M.S.D. of 0.14 Å for 290 Cα atom pairs. R.M.S.D. among the monomers of *S. pyogenes* LacD.1 and *S. aureus* LacD are 0.62–1.32 Å for 276–282 Cα atom pairs.

The monomers of *S. aureus* LacD and *S. pyogenes* LacD.1 are structurally highly similar to *S. pyogenes* LacD.2 [12], with R.M.S.D. of 0.40–0.73 Å and 0.50–1.03 Å for 282–300 and 283–298 equivalent Cα positions, respectively. They are also structurally similar to eukaryotic Class I FBP aldolases despite much lower sequence identities [13–17].

3.2. Unique dimerization of S. aureus LacD and S. pyogenes LacD.1

Our crystal structures reveal that both *S. aureus* LacD and *S. pyogenes* LacD.1 form similar dimers in the crystals with approximate dimensions of 90 Å × 55 Å × 50 Å (Fig. 1B). Between two monomers of *S. aureus* LacD dimer, the buried surface area is 1030 Å^2/monomer, corresponding to 7.1% of the monomer surface (14 440 Å^2). In the *S. pyogenes* LacD.1 dimer, a surface area of 1030 Å^2/monomer is buried at the interface between the monomers, corresponding to 7.2% of the monomer surface (14 330 Å^2). The interface between the two monomers is contributed mainly by helices α5 and α6 in both *S. aureus* LacD and *S. pyogenes* LacD.1 (Fig. 1B). The conserved dimerization mode observed in both crystals of *S. aureus* LacD and *S. pyogenes* LacD.1 suggests that these dimeric structures in the crystals likely represent the dimers in the solution.

The dimerization pattern of *S. aureus* LacD and *S. pyogenes* LacD.1 is distinct from that in the dimeric unit of Class I FBP aldolase from rabbit muscle (PDB code 6ALD), which exists as a homotetramer of 222 symmetry. The inter-subunit interface is formed mainly by β4, β5, and α7 in Class I FBP aldolase from rabbit muscle (Supplementary Fig. S2). As a result, active sites of the two monomers face toward the same side in the dimer of *S. aureus* LacD and *S. pyogenes* LacD.1 (Fig. 1B), whereas the active sites of the two monomers face toward opposite directions in rabbit muscle aldolase (Supplementary Fig. S2). Class I FBP aldolases from *Plasmodium falciparum* (1A5C), human brain (1XFB), and human liver (1QO5) also exist as structurally similar homotetramers like rabbit muscle aldolase.

3.3. Structural basis for broadened substrate specificity of Class I TBP aldolases 1

Two crystal structures of Class I TBP aldolases reported in this study provide a structural basis to understand the difference in substrate specificities between Class I TBP aldolases and Class I FBP aldolases. Superposition of rabbit muscle Class I FBP aldolase with each of *S. aureus* LacD and *S. pyogenes* LacD.1 monomers indicates that Class I TBP aldolases and Class I FBP aldolases share highly conserved active sites. In rabbit muscle FBP aldolase, the residues D33/S271/G272/G302 interact with the P1 phosphate oxyanion of FBP in two Michaelis complex structures (PDB codes 4ALD and 6ALD). These residues are structurally conserved as

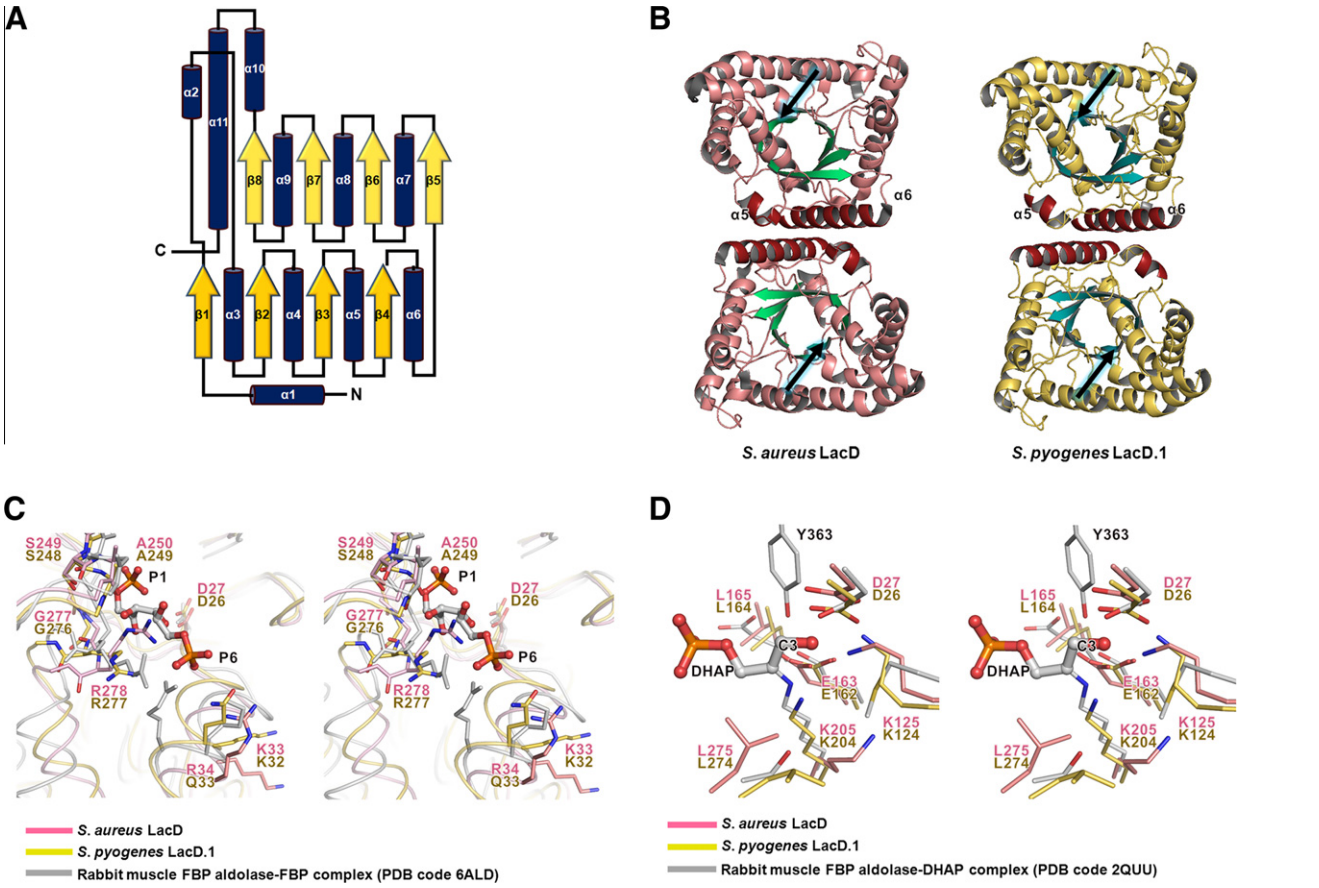

Fig. 1. Structures of Class I TBP aldolases, *S. aureus* LacD and *S. pyogenes* LacD.1, and structural comparisons with rabbit muscle Class I FBP aldolase. (A) Topology diagram of both *S. aureus* LacD and *S. pyogenes* LacD.1. α-Helices are shown as cylinders (blue) and β-strands as arrows (yellow). (B) Dimeric structure of *S. aureus* LacD (left) and *S. pyogenes* LacD.1 (right). α-Helices α5 and α6 are colored in red for both *S. aureus* LacD and *S. pyogenes* LacD.1. β-Strands are colored in green for *S. aureus* LacD and in teal for *S. pyogenes* LacD.1. The substrate binding sites inferred from a superposition with rabbit muscle Class I FBP aldolase are indicated by black arrows. (C) Stereo view of the superposition of the active site residues in *S. aureus* LacD (salmon) and *S. pyogenes* LacD.1 (yellow) with those in rabbit muscle Class I FBP aldolase (gray; PDB code 6ALD; a Michaelis complex with FBP). Structure figures were drawn using PyMOL (DeLano, W.L. (2002) The PyMOL Molecular Graphics System. DeLano Scientific, Palo Alto, CA). (D) Stereo view of the superposition of the active site residues in *S. aureus* LacD (salmon) and *S. pyogenes* LacD.1 (yellow) with those in rabbit muscle Class I FBP aldolase complexed with DHAP (gray; PDB code 2QUU).

D27/S249/A250/G277 in *S. aureus* LacD and D26/S248/A249/G276 in *S. pyogenes* LacD.1 (Fig. 1C). In a Michaelis complex structure of rabbit muscle aldolase (PDB code 6ALD), K41/R42/R303 interact with the P6 phosphate oxyanion of FBP. These residues are conserved as K33/R34/R278 in *S. aureus* LacD and K32/Q33/R277 in *S. pyogenes* LacD.1 (Fig. 1C). However, in another Michaelis complex structure of rabbit muscle aldolase (PDB code 4ALD), the P6 phosphate oxyanion of FBP binds to a different binding site (Supplementary Fig. S3). It interacts with S35/S38/K107, which are not conserved in *S. aureus* LacD and *S. pyogenes* LacD.1.

Despite strong conservation of the key active site residues between Class I TBP aldolases and Class I FBP aldolases, our structures reveal key differences that could be responsible for the broadened substrate specificity of Class I TBP aldolases compared to Class I FBP aldolases. Structural comparisons indicate that E189/S300 in rabbit muscle FBP aldolase are replaced by L165/L275 in *S. aureus* LacD and L164/L274 in *S. pyogenes* LacD.1 (Fig. 1D). E189 and S300 of rabbit muscle FBP aldolase play an important role in the proton transfer during the conversion between dihydroxyacetone phosphate (DHAP) enamine and DHAP iminium, and in the stabilization of DHAP enamine during the FBP condensation, respectively [18]. Furthermore, *S. aureus* LacD and *S. pyogenes* LacD.1 lack an equivalent residue corresponding to the C-terminal Y363 of rabbit muscle FBP aldolase. Y363 of rabbit muscle FBP aldolase performs a stereo-specific proton transfer as a mobile catalyst (Fig. 1D) [1,18]. These differences are conserved in other Class I TBP aldolases (Fig. 2).

Our structural analyses, as well as the structure of *S. pyogenes* LacD.2 [12], suggest that the substitution (or absence) of rabbit muscle FBP aldolase E189/S300/Y363 in the active sites of *S. aureus* LacD and *S. pyogenes* LacD.1 (Fig. 1D) is the most important determinant in the broadened stereo-specificity of Class I TBP aldolases as compared to Class I FBP aldolases. E189 and S300 are replaced by leucine in both *S. aureus* LacD and *S. pyogenes* LacD.1, as mentioned above. Y363 is the C-terminal residue of rabbit muscle Class I FBP aldolase and there is no counterpart in *S. aureus* LacD and *S. pyogenes* LacD.1 (Fig. 2). To test the suggestion about the role of rabbit muscle FBP aldolase E189/S300, we prepared two single mutants (L165E and L275S) and a double mutant (L165E/L275S) of *S. aureus* LacD, and compared their TBP/FBP cleavage activities with that of the wild-type. Relative to the wild-type *S. aureus* LacD, the three mutants showed enhanced preferences for FBP (Fig. 3). This result confirms that E189/S300 of rabbit muscle Class I FBP aldolase are important for shifting the substrate specificity toward FBP.

3.4. Structural insight into a possible RopB interaction with S. pyogenes LacD.1

Only *S. pyogenes* LacD.1 has an additional regulatory function on the transcription of virulence genes [9]. Overall structures of the *S.*

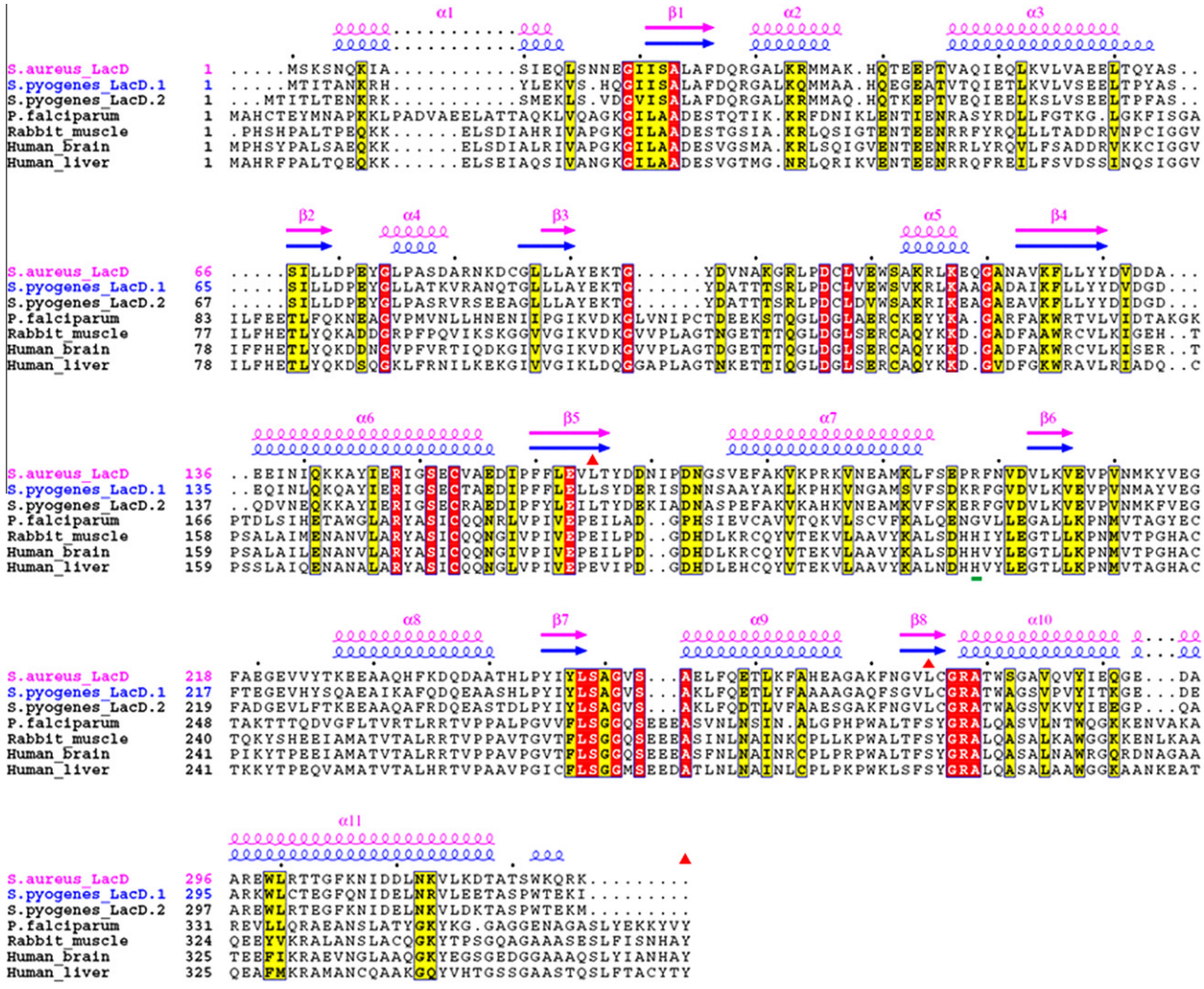

Fig. 2. Sequence alignment of Class I TBP aldolases and Class I FBP aldolases. Every tenth residue is marked with a black circle above the sequence of *S. aureus* LacD. The secondary structures of *S. aureus* LacD and *S. pyogenes* LacD.1 are colored in pink and blue, respectively. Strictly conserved residues are highlighted with red background. Semi-conserved residues are highlighted with yellow background. Seventeen residues responsible for dimeric interaction are designated by green-colored bars. Three key differences responsible for relaxed substrate specificity of TBP aldolases are indicated by red triangles. The sequences of three Class I TBP aldolases (*S. aureus* LacD, *S. pyogenes* LacD.1, and *S. pyogenes* LacD.2) and four Class I FBP aldolases (*P. falciparum*, rabbit muscle, human brain, and human liver) are aligned using the program ClustalX [21]. The figure was generated with the program ESPript [22].

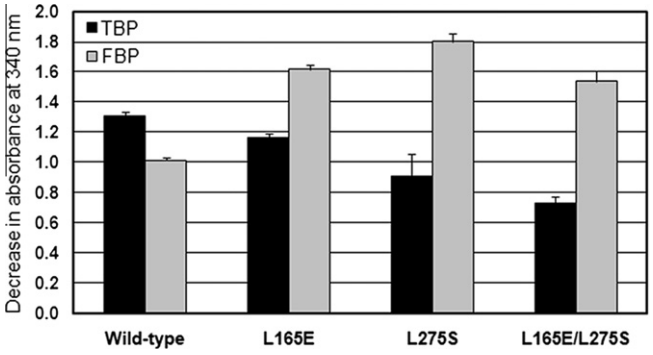

Fig. 3. TBP/FBP cleavage activities, as measured by the decrease in absorbance at 340 nm, for the wild-type and mutant enzymes (L165E, L275S, and L165E/L275S) of *S. aureus* LacD.

pyogenes LacD.1 dimer and *S. pyogenes* LacD.2 dimer are highly similar to each other, with R.M.S.D. of 0.51–0.82 Å for 570–603 equivalent Cα positions, reflecting a high level (72%) of sequence identity between them. However, a number of surface patches show noticeable differences between LacD.1 and LacD.2. These differences may be important for RopB to distinguish LacD.1 from LacD.2. As shown in Fig. 4A, the surface charge distribution around α2, α3, α10, and α11 near the active site of *S. pyogenes* LacD.1 is distinct from that of *S. pyogenes* LacD.2. Interestingly, these helices are most affected by a conformational change in *S. pyogenes* LacD.2 upon binding of DHAP [12]. The binding of DHAP to *S. pyogenes* LacD.1 was shown to induce a conformational change in such a way that its regulatory partner RopB is sequestered, thus preventing the partner from activating the target genes [9]. A previous mutational study identified G276 and R277 on α10 of *S. pyogenes* LacD.1 to be important in regulation [9]. Helices α5 and α6 of *S. pyogenes* LacD.1 and LacD.2 contribute to the dimeric interface around a twofold symmetry axis through salt bridges and hydrogen bonds (Fig. 4B).

An analysis of the dimeric interface by PISA [19] indicates that 15 residues of LacD.1 (L107, V108, E109, W110, S111, R114, A117, Q136, L139, Q142, E146, R147, S150, T153, and E155) are involved in the inter-subunit contacts in the dimer. Their corresponding residues in LacD.2 are L108, D109, V110, W111, S112, R115, E118, D137, E140, K143, E147, R148, S151, R154, and

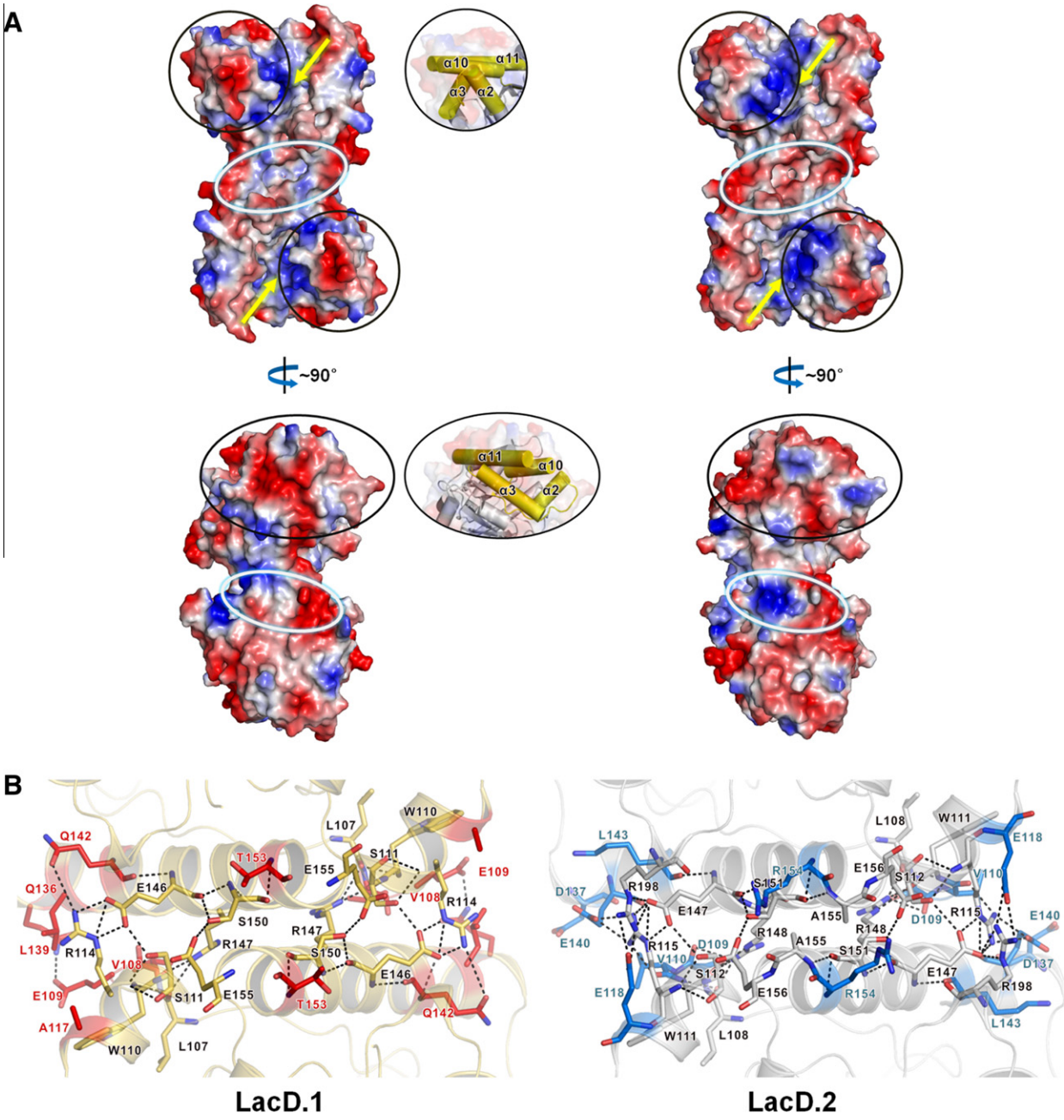

Fig. 4. Dimeric interfaces and electrostatic potential surfaces of *S. pyogenes* LacD.1 and LacD.2. (A) Electrostatic potential surface diagrams of *S. pyogenes* LacD.1 (left) and LacD.2 [12] (right) in two orientations. The molecular surface is colored in blue and red according to positive and negative electrostatic potentials, respectively. The active site cleft is indicated by yellow arrows. α2, α3, α10, and α11 are indicated by black circles. The surface regions of α5 and α6 in Fig. 1B are indicated by white circles. The surface potential diagrams were drawn using PyMOL (DeLano, W.L. (2002) The PyMOL Molecular Graphics System. DeLano Scientific, Palo Alto, CA). (B) Detailed interactions at the interface between monomers of *S. pyogenes* LacD.1 (left) and LacD.2 [12] (right). Residues conserved between LacD.1 and LacD.2 are colored in yellow (left) and gray (right), respectively. Residues unique to LacD.1 and LacD.2 are colored in red (left) and blue (right), respectively.

E156. Most of the seven variable residues (V108/E109/A117/Q136/L139/Q142/T153 in LacD.1 and D109/V110/E118/D137/E140/K143/R154 in LacD.2) are largely surface-exposed, except Q142 of LacD.1 and K143 of LacD.2 that are more buried. *S. pyogenes* RopB contains a helix-turn-helix motif at the N-terminus for DNA-binding and was shown to form a homodimer in vitro [10]. This is in general agreement with previous structural data on many prokaryotic proteins containing the helix-turn-helix motif, which bind DNA as a homodimer [20]. When the *S. pyogenes* LacD.1 dimer and the RopB dimer bind to each other to form a complex, their twofold symmetry axes may possibly be matched. However, further structural studies on their complex are necessary to confirm this suggestion.

Acknowledgements

We thank Prof. W.-D Fessner (TU Darmstadt, Darmstadt, Germany) for a generous gift of TBP. We thank the beamline staffs at Pohang Light Source, Korea (BL-4A, BL-6B, and BL-6C) and Photon Factory, Japan (BL-5A and BL-17A) for assistance during X-ray diffraction experiments. This work was funded by the Korea Ministry of Education, Science, and Technology, National Research Founda-

tion of Korea; Korea-New Zealand Cooperative Research Grant, Basic Science Outstanding Scholars Program, and World-Class University Program (Grant No. 305-20080089) and the Korea Ministry for Health, Welfare & Family Affairs (Korea Healthcare Technology R&D Project, Grant No. A092006) to SWS and by a Basic Research Promotion Grant of the Korea Research Foundation to HJY (KRF-2005-075-C00018).

Appendix A. Supplementary data

Supplementary data associated with this article can be found, in the online version, at doi:10.1016/j.febslet.2010.12.038.

References

[1] Marsh, J.J. and Lebherz, H.G. (1992) Fructose-bisphosphate aldolases: an evolutionary history. Trends Biochem. Sci. 17, 110–113.
[2] Rutter, W.J. (1964) Evolution of aldolase. Fed. Proc. 23, 1248–1257.
[3] Lorentzen, E., Siebers, B., Hensel, R. and Pohl, E. (2004) Structure, function and evolution of the Archaeal class I fructose-1,6-bisphosphate aldolase. Biochem. Soc. Trans. 32, 259–263.
[4] Bissett, D.L. and Anderson, R.L. (1980) Lactose and D-galactose metabolism in *Staphylococcus aureus*. J. Biol. Chem. 255, 8750–8755.
[5] Liotard, B. and Sygusch, J. (2004) Purification, crystallization and preliminary X-ray analysis of native and selenomethionine class I tagatose-1,6-bisphosphate aldolase from *Streptococcus pyogenes*. Acta Cryst. D60, 528–530.
[6] Cunningham, M.W. (2000) Pathogenesis of group A streptococcal infections. Clin. Microbiol. Rev. 13, 470–511.
[7] Tart, A.H., Walker, M.J. and Musser, J.M. (2007) New understanding of the group A *Streptococcus* pathogenesis cycle. Trends Microbiol. 15, 318–325.
[8] Shelburne, S.A., Davenport, M.T., Keith, D.B. and Musser, J.M. (2008) The role of complex carbohydrate catabolism in the pathogenesis of invasive streptococci. Trends Microbiol. 16, 318–325.
[9] Loughman, J.A. and Caparon, M.G. (2006) A novel adaptation of aldolase regulates virulence in *Streptococcus pyogenes*. EMBO J. 25, 5414–5422.
[10] Loughman, J.A. and Caparon, M.G. (2007) Contribution of invariant residues to the function of Rgg family transcription regulators. J. Bacteriol. 189, 650–655.
[11] Loughman, J.A. and Caparon, M.G. (2007) Comparative functional analysis of the *lac* operons in *Streptococcus pyogenes*. Mol. Microbiol. 64, 260–280.
[12] Lowkam, C., Liotard, B. and Sygusch, J. (2010) Structure of a class I tagatose-1,6-biphosphate aldolase: study into an apparent loss of stereospecificity. J. Biol. Chem. 285, 21143–21152.
[13] Choi, K.H., Mazurkie, A.S., Morris, A.J., Utheza, D., Tolan, D.R. and Allen, K.N. (1999) Structure of a fructose-1,6-bis(phosphate) aldolase liganded to its natural substrate in a cleavage-defective mutant at 2.3 Å. Biochemistry 38, 12655–12664.
[14] Kim, H., Certa, U., Döbeli, H., Jakob, P. and Hol, W.G. (1998) Crystal structure of fructose-1,6-bisphosphate aldolase from the human malaria parasite *Plasmodium falciparum*. Biochemistry 37, 4388–4396.
[15] Arakaki, T.L., Pezza, J.A., Cronin, M.A., Hopkins, C.E., Zimmer, D.B., Tolan, D.R. and Allen, K.N. (2004) Structure of human brain fructose-1,6-(bis)phosphate aldolase: linking isozyme structure with function. Protein Sci. 13, 3077–3084.
[16] Dalby, A.R., Tolan, D.R. and Littlechild, J.A. (2001) The structure of human liver fructose-1,6-bisphosphate aldolase. Acta Cryst. D57, 1526–1533.
[17] Dalby, A.R., Dauter, Z. and Littlechild, J.A. (1999) Crystal structure of human muscle aldolase complexed with fructose-1,6-bisphosphate: mechanistic implications. Protein Sci. 8, 291–297.
[18] St-Jean, M. and Sygusch, J. (2007) Stereospecific proton transfer by a mobile catalyst in mammalian fructose-1,6-bisphosphate aldolase. J. Biol. Chem. 282, 31028–31037.
[19] Krissinel, E. and Henrick, K. (2007) Inference of macromolecular assemblies from crystalline state. J. Mol. Biol. 372, 774–797.
[20] Huffman, J.L. and Brennan, R.G. (2002) Prokaryotic transcription regulators: more than just the helix-turn-helix motif. Curr. Opin. Struct. Biol. 12, 98–106.
[21] Thompson, J.D., Gibson, T.J., Plewniak, F., Jeanmougin, F. and Higgins, D.G. (1997) The CLUSTAL_X windows interface: flexible strategies for multiple sequence alignment aided by quality analysis tools. Nucleic Acids Res. 25, 4876–4882.
[22] Gouet, P., Courcelle, E., Stuart, D.I. and Métoz, F. (1999) ESPript: analysis of multiple sequence alignments in PostScript. Bioinformatics 15, 305–308.